Bacterially produced spermidine induces plant systemic susceptibility to pathogens

Ryan A. Melnyk[1#], Polina Beskrovnaya[1#], Zhexian Liu[1], Yi Song[1,2] and Cara H. Haney[1*]

Affiliations:

[1]Department of Microbiology and Immunology, The University of British Columbia, Vancouver, Canada V6T 1Z3

[2]State Key Laboratory of Genetic Engineering and Fudan Institute of Plant Biology, School of Life Sciences, Fudan University, Shanghai, China, 200438

[#]These authors contributed equally

*Correspondence: cara.haney@msl.ubc.ca

Summary

Plant root-associated microbes promote plant growth, in part by the induction of systemic resistance (ISR) to foliar pathogens. In an attempt to find novel growth-promoting and ISR inducing strains, we previously identified strains of root-associated *Pseudomonas* spp. that promote plant growth but unexpectedly induced systemic susceptibility (ISS) to foliar pathogens. Here we demonstrate that the ISS-inducing phenotype is common among root-associated *Pseudomonas* spp. and we identified the underlying genetic and molecular basis of ISS. Using comparative genomics we identified a single *P. fluorescens* locus containing a novel periplasmic spermidine biosynthesis gene *speE2* that is unique to ISS strains. We generated a clean deletion of the *speE2* gene in two ISS strains and found that *speE2* is necessary for the ISS phenotype. Spermidine but not spermine is sufficient to phenocopy ISS strains. The ISS locus is present in diverse bacteria and has previously been implicated in pathogenesis in animals. Collectively these data show that a single bacterially derived molecule can modulate systemic plant immunity.

Keywords: rhizosphere, microbiome, induced systemic susceptibility, spermidine, polyamine, *Pseudomonas*, Arabidopsis

Introduction

Plant growth promotion by beneficial microbes has long been of interest because of the potential to improve crop yields. Individual root-associated microbial strains can promote plant growth by facilitating nutrient uptake, producing plant hormones, or improving resilience to both abiotic and biotic stresses [1]. In some cases, single bacterial loci underlie beneficial effects of microbes on plants while other traits appear to be complex and polygenic.

Pseudomonas fluorescens and related species are a model for beneficial host-associated microbes due to their genetic tractability and robust host-association across diverse eukaryotic hosts. Direct plant growth promotion (PGP) by *Pseudomonas* spp. can be mediated by bacterial production of the phytohormones auxin [2] or by the expression of 1-aminocyclopropane-1-carboxylate (ACC) deaminase that metabolizes plant-derived ethylene [1,3]. Indirect PGP through antimicrobial activity and pathogen suppression has been attributed to production of the antibiotic 2,4-diacetylphloroglucinol (DAPG) [4]. However, the molecular basis of many traits such as induced systemic resistance (ISR) has remained elusive, and multiple distinct bacterial traits including production of siderophores, LPS, and salicylic acid have all been implicated [5].

We previously reported two *Pseudomonas* spp. that induce systemic susceptibility (ISS) on *Arabidopsis* and can promote growth under nutrient limiting conditions [6,7]. These same *Pseudomonas* strains suppress a subset of SA-dependent responses and promote resistance to herbivores [7]. Although it is possible that these strains contain multiple genetic loci that affect plant growth and pathogen resistance, we were interested in investigating whether a single bacterial trait is primarily responsible for both growth and immunity phenotypes. Growth and immunity have a reciprocal relationship in plants, leading to growth-defense tradeoffs to the extent that plant stunting has been used as a proxy for autoimmunity [8]. As a result, we

hypothesized that suppression of plant immunity by *Pseudomonas* strains that trigger ISS may be a consequence of PGP activity. The genomes of these strains do not contain genes for the ACC deaminase enzyme prevalent in other *Pseudomonas* PGP strains [3]; thus, we hypothesized that there may be a distinct mechanism of growth promotion in these strains.

Because of the high density of sampling and genome sequencing within *P. fluorescens* and related species, we reasoned that if ISS is an overlooked consequence of growth promotion then: 1) we should be able to identify additional ISS strains by sampling known PGP strains and additional root-associated strains, and 2) assuming a single unique locus was responsible, that a comparative genomics approach should reveal the underlying genetic basis of ISS.

Here we report that ISS is relatively common among *Pseudomonas* strains. We identified new ISS isolates including previously described PGP or environmental isolates and new isolates from *Arabidopsis* roots. Using comparative genomics, we identified a single bacterial locus containing a spermidine synthase gene (*speE2)* that is unique to *Pseudomonas* ISS strains. We show that *speE2* is necessary to elicit ISS and that exogenous spermidine is sufficient to trigger ISS in the absence of bacteria. Collectively, these data indicate that a single monogenic microbial trait underlies a systemic immune response in a plant host.

Results

ISS is a common feature of growth-promoting *Pseudomonas* spp.

We previously reported that two strains of *Pseudomonas* (CH229 and CH267) induce systemic susceptibility (ISS) to the foliar pathogen *Pseudomonas syringae* DC3000 (*Pto* DC3000) under conditions where a well characterized ISR strain (*P. simiae* WCS417 [9]) conferred resistance to *Pto* DC3000 [6,7]. To the best of our knowledge, descriptions of *Pseudomonas*-elicited ISS

against bacterial pathogens are limited to *Pseudomonas* sp. CH229 and CH267, strains that were independently isolated from the rhizospheres of wild *Arabidopsis* plants in Massachusetts, USA. We reasoned that if ISS is common among *Arabidopsis*-associated *Pseudomonas* spp., we would be able to identify additional ISS strains from *Arabidopsis* roots from plants growing at distinct sites.

We isolated 25 new fluorescent pseudomonads from wild-growing *Arabidopsis* plants from additional sites in Massachusetts and in Vancouver, Canada. We generated ~800 bp sequences of a region of the 16S rRNA gene where strains CH229 and CH267 are 99.5% identical, but each shares only <96% identity to the well-characterized ISR strain WCS417. Reasoning that new ISS strains would be closely related to CH267 and CH229, we selected 3 new isolates [1 from Massachusetts (CH235) and 2 from British Columbia (PB101 and PB106)] that were >97% identical to CH267 by 16S rRNA sequence and another 3 (from British Columbia: PB100, PB105 and PB120) that were <97% identical to CH229 and CH267 (Figure 1A).

We tested these 6 new rhizosphere *Pseudomonas* isolates for their ability to trigger ISS. We found that 2 of the 3 strains that were most closely related to CH267 (CH235 and PB101) elicited ISS (Figure 1B). Two strains with <96% identity to CH267 failed to trigger ISS: PB105 triggered ISR and PB100 had no effect on systemic defenses (Figure 1). PB106 and PB120 consistently enhanced susceptibility in all experiments, but to a more moderate degree (*$p<0.1$). Collectively, these data indicate that the ability to elicit ISS on *Arabidopsis* ecotype Col-0 may be a common feature among some, but not all, closely-related strains of *Pseudomonas* spp. isolated from the *Arabidopsis* rhizosphere.

Because ISS seemed restricted to strains that were closely related to CH267, we obtained several additional isolates with similar 16S sequences including *Pseudomonas* sp. UW4, *Pseudomonas* sp. Pf0-1 and *P. vancouverensis* DhA-51 (Table 1) and a growth promoting strain, *Pseudomonas* sp. WCS365, that is more distantly related and to our knowledge has not been tested for ISR/ISS. We found that UW4 and DhA-51 elicited ISS while Pf0-1 and WCS365 did not (Figure 1B). *Pseudomonas* sp. UW4 [10] and WCS365 are well-characterized growth promoting strains. *Pseudomonas* sp. Pf0-1 [11] is an environmental isolate. *Pseudomonas vancouverensis* DhA-51 is also an environmental isolate [12] and was previously shown to be closely related to Pf0-1 [13]. Because DhA-51 is an environmental isolate that triggers ISS, these data show that the ability to trigger ISS is not specific to rhizosphere isolates.

To gain insights into the distinguishing features of ISS strains, we sequenced the genomes of the 6 new isolates (CH235, PB100, PB101, PB105, PB106 and PB120) from *Arabidopsis* roots as well as *P. vancouverensis* DhA-51 (UW4, WCS365, CH267 and CH229 have been sequenced previously). Whole genome shotgun sequencing was used to assemble draft genomes (Methods). We generated a phylogenetic tree using 122 conserved genes as described previously [7,14]. We found that all ISS strains are closely related to one another and fall within a monophyletic group which corresponds to the *P. koreensis, P. jessenii,* and *P. mandelii* subgroups of *P. fluorescens* identified in a recent phylogenomic survey of *Pseudomonas* spp. (Figure 2B; [15]). However, not every isolate in this clade is an ISS strain; notably Pf0-1, which has no effect on systemic immunity despite being closely related to CH229. We reasoned that the absence of the ISS phenotype in Pf0-1 should facilitate the use of comparative genomics by allowing us to separate the phylogenetic signature from the phenotypic signature of ISS.

11 genes in a single genomic locus are unique to ISS strains and predicts ISS

To identify the potential genetic basis of the ISS phenotype, we used a previously described database of orthologous genes for *Pseudomonas* spp. [14] to identify genes that are present in ISS strains (CH229, CH235, CH267 and UW4) but are absent in the closely-related strain that has no effect on systemic defenses (Pf0-1). We used only the ISS strains with the most robust phenotypes for this analysis. We identified 29 predicted protein coding genes missing from Pf0-1 but present in all of the other strains. Of these, 12 were small (<100 aa) hypothetical proteins. The remaining 17 predicted protein coding genes were prioritized for further analysis and are shown in S1 Table. Intriguingly, 11 of the 17 ISS unique genes are found in a single genomic locus.

We surveyed the genomes of other *Pseudomonas* strains tested for ISS to determine if the presence of the 17 genes identified by our comparative genomics approach correlated with the ISS phenotype. We found that the 11 clustered genes were present in ISS strains (DhA-51 and PB101) and the strains with intermediate phenotypes (PB120 and PB106) but were absent in the non-ISS strain WCS365, WCS417 and PB105 (S1 Figure). The remaining 6 genes were all present in WCS365 and/or other non-ISS strains (S1 Figure). We chose to focus on the 11 ISS-unique genes ("ISS locus" hereafter) for further study.

We found that the 11 genes in the ISS locus are found at a single genomic locus in all 4 of the ISS strains (S2 Figure and Figure 2A). The flanking regions are conserved in the non-ISS strain Pf0-1 (Figure 2A), indicating a recent insertion or deletion event. Within this locus, there is a single gene that is conserved in Pf0-1 in addition to two genes that are unique to each individual strain suggesting multiple changes to this genomic region in recent evolutionary

history. While all 11 genes are within the same genomic region in the ISS strains, the variability of this locus between closely related strains suggests it may be rapidly evolving.

We surveyed the genomes of sequenced isolates available in our collection for the presence of the ISS locus. We found a number of closely-related strains from various environmental sources that contained the ISS locus, as well as a more distantly related strain (Pf-5) (Figure 2B). We tested 2 of these newly identified strains that contain the ISS locus (Pf-5 and GW456-L13) as well as 2 that do not (FW300-N1B4 and FW300-N2C3) and found that the presence of the ISS locus correlated with the ISS phenotype, including the distantly related strain Pf-5 (Figure 2C). Collectively, these data show that the presence of the 11 candidate genes in the ISS locus identified by our comparative genomics approach is predictive of the ISS phenotype.

SpeE is necessary and spermidine is sufficient to trigger ISS

Because ISS strains CH267 and CH229 have previously been shown to promote growth [6], we examined the annotations of the 11 genes within the ISS locus for a gene that might be involved in biosynthesis of a growth-promoting or immuno-modulatory compound (Figure 2A). We identified a predicted polyamine synthase-encoding gene within the ISS locus annotated as *speE2* (PputUW4_02826 and CP336_12795 in UW4 and CH267 respectively). CH267 *speE2* has similarity to a characterized spermidine synthase gene *speE* in *P. aeruginosa* (25% predicted amino acid identity to *P. aeruginosa* PA1687 [16]). A second *speE*-like genes in the genomes of UW4 and CH267 annotated as *spE1* is outside of the ISS locus (PputUW4_03691 and CP336_28780 in UW4 and CH267 respectively) and is highly similar to the *P. aeruginosa speE* gene (~84.0% predicted amino acid identity) [16]. Polyamines including spermidine have been

166 implicated in a range of plant growth and defense-related phenotypes [17,18] and are known to
167 be synthesized by diverse microbes [19].

168 To test if the gene cluster and the *speE2* gene are necessary for ISS strains to induce
169 systemic susceptibility, we deleted the entire 15 kB locus including the region spanning the 11
170 genes identified in our initial comparative genomics screen in strains CH267 and UW4 (Figure
171 2A). We also constructed an in-frame deletion of just the *speE2* gene in both CH267 and UW4.
172 We retested these deletion mutants for their ability to induce systemic susceptibility and found
173 that deletion of the *speE2* gene alone, or the entire 11-gene cluster, resulted in a loss of the ISS
174 phenotype in both CH267 and UW4 (Figure 3A). This indicates that *speE2* is necessary for ISS.

175 To determine if spermidine or a related polyamine is sufficient to trigger ISS, we watered
176 soil-grown plants with purified spermidine or spermine at concentrations of 1, 10 and 100 µM.
177 Spermidine application in this range has been previously shown to promote plant salt tolerance
178 [20]. We found that 10 and 100 µM spermidine but not spermine could induce systemic
179 susceptibility indicating that spermidine is sufficient to phenocopy the bacterial ISS phenotype
180 (Figure 3B).

181

182 **_speE2_ is a predicted periplasmic spermidine synthase that uses a novel source of dSAM**

183 Because deletion of *speE2* in CH267 and UW4 results in the specific loss of the ISS phenotype,
184 this indicates that the *speE1* and *speE2* genes are not functionally redundant. *SpeE1* and *speE2*
185 differ in length and predicted structure (Figure 4A). *SpeE1* encodes a predicted 384-amino acid
186 protein and contains a predicted polyamine synthase domain with a predicted decarboxylated S-
187 adenosyl methionine (dSAM) binding motif. *SpeE2* encodes a protein of a predicted 847 amino
188 acids. The C-terminus of *speE2* contains the same dSAM domain as *speE1* but also contains

predicted transmembrane domains at its N-terminus. Using a transmembrane domain prediction and protein localization tool, TMHMM, we found that the SpeE2 protein has a total of 13 predicted transmembrane helices [21]. We found that the spermidine synthase domain of SpeE2 is predicted to be in the periplasm (Figure 4B). This suggests that SpeE2 may represent a novel class of periplasmic spermidine synthase proteins.

Because the cytoplasmic *speE1* gene cannot complement ISS activity in a *speE2* mutant of CH267 or UW4, we wondered if there are cognate periplasmic variants of the remainder of the canonically cytoplasmic spermidine synthase pathway. Spermidine biosynthesis can occur via two known pathways (Figure 4C). The first, by *speE,* occurs when the aminopropyl group of dSAM is transferred to putrescine. SAM decarboxylation to dSAM occurs via *speD* [16]. The second spermidine synthase pathway is independent of *speDE* and converts putrescine to spermidine by a carboxyspermidine intermediate via a dehydrogenase (*CASDH*) and a decarboxylase (*CASDC*) [22]. Because *speE2* also contains a predicted dSAM binding motif, this suggests that a dSAM biosynthesis gene should also be present in the genomes of ISS strains.

We surveyed the genomes of ~3800 sequenced *Pseudomonas* isolates for the presence of *speD, speE, CASDH* and *CASDC* and found that the majority of strains contained genes for either the *speD/E1* cytoplasmic spermidine biosynthetic pathway or the *CASDH/C* biosynthetic pathway (Figure 4E shows the same set of strains shown in Figure 2). We generated a Pearson correlation matrix of the co-occurrence of spermidine biosynthesis genes. We found a near perfect correlation of components within each of the two known biosynthetic pathways (*speD/speE1* and *CASDH/C*). Interestingly, there was a nearly perfect anti-correlation between the presence of the *speD/speE1* and *CASDH/C* pathways (Figure 4D). This suggests that nearly all *Pseudomonas* make spermidine cytoplasmically, but they do it either via *speD/E* or via

CASDH/C and do not contain both pathways. These pathways are both polyphyletic, as there are examples of sister clades containing opposite pathways, both at the species level (S3 Figure) and within the *P. fluorescens* subclade (S4 Figure).

dSAM is required as a precursor to synthesize spermidine via *speE*. We could not identify a dSAM biosynthesis gene in any of our strains that has a predicted periplasmic localization. Moreover, while most strains with *speE2* contain *speD/E1* genes, *Pseudomonas* spp. PB106, PB120 and Pf-5 do not (Figure 4E). Beyond the strains we characterized, there was a weak negative correlation at the genus level between *speD/E1* and *speE2* (Figure 4D) indicating that strains that contain an *speE2* gene do not necessarily contain *speD*. Because *speE2* has a predicted dSAM binding domain, the source of the dSAM needed to catalyze spermidine production in strains lacking *speD* is elusive. These data suggest that *speE2* must work with a novel dSAM biosynthesis gene to synthesize spermidine, generate spermidine in a dSAM-independent manner, or use an external source of dSAM, either from a eukaryotic host, or from other members of a bacterial community.

Additional roles for the ISS locus in host interactions

While *speE2* is necessary for ISS, we wondered if the other 10 genes in the ISS locus are also involved in interactions with a plant host. We tested whether the pattern seen in Figure 4D, where *speE2* is always associated with the same larger locus, would hold up across the genus *Pseudomonas*. When we analyzed our entire computational dataset of >3800 genomes from across *Pseudomonas*, we found that there was a strong correlation for the presence or absence of 9 of 11 genes ($r > 0.9$, Figure 5A). Moreover, we also found that these 9 co-occurring genes were frequently found in the same genomic region, as there were moderate to strong correlations for 9

of the 11 genes co-occurring in the same 50-kb genomic region (Figure 5B). From a phylogenomic standpoint, we found that these genes were broadly distributed throughout the *Pseudomonas* genus and co-occurred even in taxonomic groups far outside of the *P. fluorescens* clade (Figure 5C). Within the *P. fluorescens* clade, the ISS locus genes are frequently found in some clades, such as the *koreensis* and *jessenii* clades, which contain most of our isolates (Figure 5D). However, some clades are missing these genes entirely, such as the plant associated *corrugata* clade (Figure 5D). Together, these genomic data indicate that despite their polyphyletic distribution among divergent clades of *Pseudomonas* spp., these genes likely participate in conserved or similar functions.

Beyond the predicted role of SpeE2 as a spermidine synthase, the specific functional roles of genes in this locus are less clear. We identified an operon with 6 of the genes in the ISS locus with identical domain structure and organization that is involved in stress resistance and virulence in *Francisella tularensis* [23] (Figure 6). Another similar operon is associated with aerotolerance and virulence in *Bacteroides fragilis* [24]. Returning to our comparative genomics database, we found that these 6 genes comprise an operon broadly conserved in the *Pseudomonas* clade that is distinctly paralogous from the ISS operon (Figure 6). This raises the possibility that these six genes within the ISS locus contribute to host-bacterial interactions across diverse bacterial taxa and both plant and animal hosts (Figure 6).

Discussion

Plant root-associated (“rhizosphere”) microbes perform a diversity of functions that benefit their plant hosts including nutrient uptake and defense. Functional characterization of individual plant-associated bacterial and fungal strains of potential agronomic importance (i.e.

258 growth promoters or nitrogen fixers) is widespread [5]. However, closely-related strains of
259 bacteria can have very distinct effects on plant growth and defense [13], and these effects can be
260 dependent on environmental context [1]. Lack of known correlations between microbial
261 genotype and potential effects on plant hosts present a challenge when attempting to infer the
262 effect that a microbe may have on its plant host from sequence identity alone.

263 Our use of comparative genomics and isolate phenotyping to identify the genetic basis of
264 a complex microbial-derived trait indicates that this is an effective approach to identifying
265 important microbial traits to improve plant health. For comparative genomics to be effective,
266 traits should be controlled by single or limited genomic loci, and phylogeny should not be
267 predictive of function. In this case, a close relative of ISS strains, *Pseudomonas* sp. Pf0-1 (>99%
268 identical by full length 16S rRNA to the ISS strains) does not affect systemic defenses (Figure
269 1), which allowed us to use comparative genomic to identify the underlying basis. We previously
270 used this approach to find the genomic basis of a pathogenic phenotype within a clade of
271 commensals [14]. It has been previously observed that phylogeny is not predictive of function
272 for ISR strains [13] suggesting that comparative genomics may be appropriate to find the basis of
273 additional plant-associated traits.

274 Why spermidine applied to plant roots suppresses systemic immunity is not clear; the
275 most direct role for polyamines in immunity is through oxidation and generation of reactive
276 oxygen species (ROS) that promote immunity [25,26]. Spermine has been shown to modulate
277 expression of redox and defense-related gene expression [27] and polyamines including
278 putrescine, spermine and spermidine accumulate during pathogen infection [28]. Spermidine,
279 spermine and related molecules can enhance resistance to pathogens in both plants and animals
280 through breakdown via oxidases that result in generation of ROS [25,26]. *P. syringae* promotes

generation of acetylated putrescine rather than spermidine, which is not readily oxidized and results in reduced ROS production and enhanced susceptibility [28]. We previously showed that the ISS strain CH267 suppresses a subset of SA-dependent gene expression and that ISS is SA-dependent [7]. As spermidine uptake should directly enhance resistance through accumulation of ROS, it seems more likely that spermidine applied to roots suppresses defense signaling through modulating local or systemic defense responses rather than direct uptake.

Similarly, the adaptive role of spermidine production by host-associated *Pseudomonas* remains to be determined. We and others previously showed that the polyamine putrescine promotes biofilm production in *Pseudomonas* and bacterial intracellular accumulation of putrescine inhibits rhizosphere fitness [29]. Spermidine can promote biofilm formation in *Bacillus* [30]. Our data show that predicted spermidine biosynthesis is perfectly conserved through the genus *Pseudomonas*, although there is a clear anti-correlation between the *speD/E* and *CASDH/C* pathways. The *speE2* gene shows polyphyletic inheritance and occurs in diverse *Pseudomonas* spp. (Figure 5C). The evolutionary and ecological pressures that result in *speE2* promoting bacterial fitness have yet to be elucidated.

The SpeE2 enzyme affects the plant host presumably by producing secreted spermidine, and the protein is predicted to lie within the periplasm (Figure 4A). A periplasmic localization might position the enzyme to utilize exogenous dSAM and convert either an internal or external supply of putrescine to spermidine. Complementarity of biosynthetic processes has been shown in other systems. For example, although most bacteria use cobalamins as enzyme cofactors, the majority do not have the ability to synthesize them [31]. While it is possible that a novel *speD* gene is present in the genomes of *speE2*-containing strains, it is possible that spermidine

biosynthesis via *speE2* might occur with an exogenous supply of dSAM, such as from a plant or another member of the microbial community.

While enhancement of systemic susceptibility is not an obviously agronomically useful plant trait, spermidine has been studied for its role in improving drought tolerance [17,20]. Additionally, several ISS strains promote growth and enhance resistance to insect pests [6,7]. Using ISS strains or spermidine might be beneficial for crops where drought or insects are the primary pressure on crop productivity. However, ISS illustrates the complexity of host microbe interactions and should be considered when engineering the microbiome.

Materials and Methods

Plant growth conditions

For all experiments, plants were grown in Jiffy-7 peat pellets (Jiffy Products) under a 12 h light/12 h dark at 22 °C temperature regime. Seeds were surface sterilized by washing with 70% ethanol for 2 minutes followed by 5 minutes in 10% bleach and 3 washes in sterile water. Seeds were stored at 4^{o} C until use. Unless otherwise indicated, seeds were sowed in Peat pellets (Jiffy 7) and placed in a growth chamber under 12-hour days and 75 μM cool white fluorescent lights at 23^{o} C.

Bacterial growth and 16S rRNA sequencing

Pseudomonas strains were cultured in LB or King's B at 28 °C. New *Pseudomonas* strains were isolated from the roots of wild-grown *Arabidopsis* plants around eastern Massachusetts, USA and British Columbia, Canada as described [6]. New *Pseudomonas* isolates were preliminary identified based on fluorescence on King's B and confirmed by 16S rRNA sequencing.

Strain	Genus and species	Isolated From	Location	Reference
CH267	*Pseudomonas* sp.	*Arabidopsis* rhizosphere	Cambridge, MA USA	[6]
CH235	*Pseudomonas* sp.	*Arabidopsis* rhizosphere	Carlisle, MA USA	[6]
CH229	*Pseudomonas* sp.	*Arabidopsis* rhizosphere	Carlisle, MA USA	[6]
PB100	*Pseudomonas* sp.	*Arabidopsis* rhizosphere	Vancouver, BC Canada	This study
PB101	*Pseudomonas* sp.	*Arabidopsis* rhizosphere	Vancouver, BC Canada	This study
PB105	*Pseudomonas* sp.	*Arabidopsis* rhizosphere	Vancouver, BC Canada	This study
PB106	*Pseudomonas* sp.	*Arabidopsis* rhizosphere	Vancouver, BC Canada	This study
PB120	*Pseudomonas* sp.	*Arabidopsis* rhizosphere	Eastham, MA USA	This study
WCS417	*P. simiae*	Wheat rhizosphere	Netherlands	[32]
UW4	*Pseudomonas* sp.	Reeds	Waterloo, ON Canada	[10]
Pf0-1	*Pseudomonas* sp.	Environmental soil		[11]
DhA-51	*P. vancouverensis*	Environmental soil	Vancouver, BC Canada	[12]
WCS365	*Pseudomonas* sp.	Tomato rhizosphere	Netherlands	[33]
Pf-5	*Pseudomonas* sp.	Cotton rhizosphere	College Station, TX USA	[34]
GW456-L13	*P. fluorescens*	Groundwater	Oakridge, TN USA	[35]
FW300-N1B4	*P. fluorescens*	Groundwater	Oakridge, TN USA	[35]
FW300-N2C3	*P. fluorescens*	Groundwater	Oakridge, TN USA	[35]

Table 1. Bacterial strains used in this study

ISS assays

ISS and ISR assays were performed as described [7]. Briefly, *Pseudomonas* rhizosphere isolates were grown at 28 °C in LB medium. For inoculation of plant roots for ISR and ISS assays, overnight cultures were pelleted, washed with 10 mM $MgSO_4$ and resuspended to a final OD_{600} of 0.02. Jiffy pellets were inoculated 9 days after seed germination with 2 mls of the indicated bacterial strains at a final OD_{600} of 0.02 ($5x10^5$ CFU g^{-1} Jiffy pellet). For spermidine and spermine treatments, 10 mM stocks were kept frozen until just before use. Just prior to use, they were diluted to the indicated concentration in water and 2 mLs were applied to the soil surrounding 3-week old plants.

For infections, the leaves of 5-week old plants were infiltrated with *Pto* DC3000 at an OD_{600} = 0.0002 (starting inoculum ~10^3 CFU/cm^2 leaf tissue). Plants were maintained under low

light (<75 µM) and high humidity for 48 hours. Leaf punches were harvested, ground, and plated to determine CFU counts.

16S rRNA sequencing, bacterial genome sequencing, assembly and phylogenomics

Bacterial DNA preps were performed using Qiagen Purgene Kit A. 16S rRNA was amplified using 8F and 1391R and sequenced using 907R.

Bacterial genomic library prep and genome sequence was performed as described [7]. Briefly, bacterial DNA was isolated using Qiagen Purgene Kit A and sonicated into ~500 bp fragments. Library construction was performed as described [7], individually indexed and sequenced using MiSeq V3 paired end 300 bp reads.

After barcode splitting, approximately 500,000 to 1 million reads were used for each sample to assemble draft genomes of the ISS strains *Pseudomonas* sp. CH235, PB100, PB101, PB103, PB105, PB106, PB120 and *P. vancouverensis* DhA-51. Genome assembly was carried out as previously described [7] and draft genomes are available from NCBI (see below).

Phylogenomic tree building

To generate the 29-taxon species tree used in Figures 2B and 4E, we made use of an alignment of 122 single-copy genes we previously found to be conserved in all bacteria [14]. From this amino acid alignment, we extracted 40,000 positions ignoring sites where >20% of the taxa had gaps. Using RAxMLv8.2.9, we inferred 20 independent trees under the JTT substitution model using empirical amino acid frequencies and selected the one with the highest likelihood. Support values were calculated through 100 independent bootstrap replicates under the same parameters.

To build the 3,886-taxon phylogeny of the *Pseudomonas* genus in Figures 5C and S1, the same 122-gene alignment was used. For computational feasibility, the alignment was randomly subsampled to 10,000 amino acid positions, again ignoring sites that were highly gapped (>20%). FastTree v2.1.9 was used to build the phylogeny using default parameters. The phylogeny was rooted to a clade of *Pseudomonas* identified as an outgroup to all other *Pseudomonas* spp. as previously described [14]. To more easily visualize this tree, we collapsed monophyletic clades with strong support (as determined by FastTree's local Shimodaira-Hasegawa test) that correspond with major taxonomic divisions identified by Hesse et al. (2018).

To build the tree for the *Pseudomonas fluorescens* (*Pfl*) subclade seen in Figures 5D and S2, we identified 1,873 orthologs specific to the *Pfl* clade found in >99% of all strains in the clade and then aligned them all to the hidden Markov models generated by PyParanoid using hmmalign, prior to concatenation. This alignment had 581,023 amino acid positions, which we trimmed to 575,629 positions after masking sites with >10% of taxa with gaps. From this alignment, we randomly subsampled 120,000 sites for our final phylogenomic dataset. Using RAxMLv8.2.9, we inferred 20 independent trees under the JTT substitution model using empirical amino acid frequencies and selected the one with the highest likelihood. Support values were calculated through 100 independent bootstrap replicates under the same parameters.

Comparative Genomics

Comparative genomics analyses were performed by using our previously described framework for identifying PyParanoid pipeline and the database we built for over 3800 genomes of *Pseudomonas* spp. Briefly, we had previously used PyParanoid to identify 24,066 discrete groups of homologous proteins which covered >94% of the genes in the original database. Using

these homolog groups, we annotated each protein-coding sequence in the newly sequenced and merged the resulting data with the existing database, generating presence-absence data for each of the 24,066 groups for 3,886 total *Pseudomonas* genomes.

To identify the groups associated with induction of systemic susceptibility, we compared the presence-absence data for 4 strains with ISS activity (*Pseudomonas* spp. CH229, CH235, CH267, and UW-4) and 1 strain with no activity (*Pseudomonas* sp. Pf0-1). We initially suspected that ISS activity was due to the presence of a gene or pathway (i.e. not the absence of a gene) and thus initially focused on genes present only in Pf0-1. We identified 29 groups that were present in the 4 ISS strains but not in Pf0-1.

To obtain the correlation coefficients in Figs. 4D and 5A, we coded group presence or absence as a binary variable and calculated Pearson coefficients across all 3,886 genomes. To calculate the correlation coefficients in Fig. 5B, we split the genomic database into 50-kb contiguous regions and assessed group presence or absence within each region. Because this dataset is heavily zero-inflated, we ignored regions that had none of the 11 groups, taking the Pearson coefficient of the 11 genes over the remaining regions.

Initial annotation of the ISS groups was based on generic annotations from GenBank Further annotation of the 11 groups specific to the ISS locus was carried out using the TMHMM v2.0 server, the SignalP 4.1 server and a local Pfam search using the Pfam-A database from Pfam v31.0. To identify homologous genes in the genomes of *Francisella tularensis* subsp. *holarctica* and *Bacteroides fragilis* YCH46, we relied on locus tags reported in the literature which we confirmed using annotation based on another Pfam-A domain search.

Deletion of the *speE2* gene and gene clusters

Deletions in the CH267 and UW4 strains were constructed by a two-step allelic exchange as described [29]. The flanking regions directly upstream and downstream of the spermidine biosynthesis cluster or the *speE* gene were amplified and joined by overlapping polymerase chain reaction (PCR) using genomic DNA as template and primers listed in Table 2. Following digest, the product was ligated into the pEXG2 suicide vector that contains the *sacB* gene for counter-selection on sucrose [36]. The recombinant plasmid was then transformed into calcium-competent *E. coli* DH5α by heat shock. After confirmation of correct insert by PCR and sequencing, the plasmid was transformed into WM3064 [37]. Conjugation of plasmid into CH267 and UW4 from WM3064 was performed by biparental mating on King's B media supplemented with diaminopimelic acid, and transconjugants were selected using 10 µg/mL gentamicin and 15 µg/mL nalidixic acid. The second recombination leading to plasmid and target DNA excision was selected for by using sucrose counter-selection. Gene deletions in CH267 and UW4 were confirmed by PCR amplification of the flanking regions with primers listed in Table 2, agarose gel electrophoresis and Sanger sequencing.

Table 2. Primers used to generate the mutant *Pseudomonas* strains analyzed in this study.

Strain	Primer type	Primer name	Restriction site	Sequence (5'→3')
CH267 Δcluster	Upstream forward	CH409	HindIII	AAAAAGCTTAGTCGCAACCTCGCCTCGACTGAC
	Upstream reverse	CH410	—	AAACGGGCGGGAGCAGCACTTGG
	Downstream forward	CH411	—	CACTGACTCCGCTTATTGTTTTGTGTC
	Downstream reverse	CH412	EcoRI	AAAGAATTCTTCACGCCGCCGCAGGATGTC
	Upstream confirmation	PB401	—	CGCTATGACCTGGGCCGCAACGAA
	Downstream confirmation	PB402	—	CCGACGCCGACCATGAGCGAAA
CH267 Δ*speE*	Upstream forward	CH413a	HindIII	AAAAAGCTTGCTCCAGCAAAACCGTCGCTCCA
	Upstream reverse	CH414a	—	CTCTCGTCATCCGATCATTCCCACGCGG
	Downstream forward	CH415	—	GAATGATTGTTCCCATGCATAGCGTGG
	Downstream reverse	CH416a	EcoRI	AAAGAATTCCCGGGCTCGACTGGTTCCCGA
	Upstream confirmation	PB403	—	CTACAGCCAACTCAAGGAGGCCAA
	Downstream confirmation	PB404	—	CGGGTGAGGTCTCGAACGAGATGT
UW4 Δcluster	Upstream forward	CH401	HindIII	AAAAAGCTTACGCCTCGGCCATCGGTGTACC
	Upstream reverse	CH402	—	GAAAGGCTCCTGCAGAAGATCGAAC
	Downstream forward	CH403	—	GTAACACCTCCAAACGTTCCGGGAT
	Downstream reverse	CH404	EcoRI	AAAGAATTCAACGCACCTGCACATCGGCTGCG

	Upstream confirmation	PB405	—	GGGTCATGTCCCTGACCAGCA
	Downstream confirmation	PB406	—	GGGTCGAATTCCGTGTCGCCAA
UW4 Δ*speE*	Upstream forward	CH405	HindIII	AAAAAGCTTGAGCCGATTGAGCTGGATGCGG
	Upstream reverse	CH406	—	TACGACTTCCATGGTCCAGGTGCG
	Downstream forward	CH407	—	TCGGGGGGCTGGCTCAAAGG
	Downstream reverse	CH408	EcoRI	AAAGAATTCACGAGTCGGCGCTCAAACGCG
	Upstream confirmation	PB407	—	CGCGAACCTGTGGACCAGCGAGTT
	Downstream confirmation	PB408	—	CGCGAACCGCGCTGCAAGAA

Acknowledgements

This work was supported by an NSERC Discovery Grant (NSERC-RGPIN-2016-04121) awarded to C.H.H., a Life Sciences Research Foundation Fellowship from the Simons Foundation awarded to R.A.M., a fellowship from China Postdoctoral Science Foundation awarded to Y.S., and an NSERC CGS-M award to Z. L.

Author Contributions

C.H., R.A.M., and P.B. designed experiments. P.B. Y.S. and C.H.H. performed experiments. C.H., R.A.M., X. L. analyzed data. and R.A.M. performed genome assembly, annotation, phylogenetic analysis and comparative genomics. C.H.H., P.B. and R.A.M. wrote the manuscript with input from all.

Data Availability

Data for the Whole Genome Shotgun project has been deposited at DDBJ/ENA/GenBank under the accessions RRZJ00000000 (CH235), RRZK00000000 (DhA-51), RWIL00000000 (PB103), RWIM00000000 (PB106), RWIN00000000 (PB120), RWIO0000000 (PB105), RWIQ00000000 (PB100), and RWIR00000000 (PB101). The versions described in this paper

445 are versions RRZJ01000000 (CH235), RRZK01000000 (DhA-51), RWIL01000000 (PB103),
446 RWIM01000000 (PB106), RWIN01000000 (PB120), RWIO0100000 (PB105), RWIQ01000000
447 (PB100), and RWIR01000000 (PB101).
448
449 **Declaration of interests:** The authors declare no competing interests.
450
451
452 **References**
453
454 1. Vacheron J, Desbrosses G, Bouffaud M-L, Touraine B, Moënne-Loccoz Y, Muller D, et
455 al. Plant growth-promoting rhizobacteria and root system functioning. Front Plant Sci.
456 Frontiers; 2013;4: 356. doi:10.3389/fpls.2013.00356
457 2. Spaepen S, Vanderleyden J, Remans R. Indole-3-acetic acid in microbial and
458 microorganism-plant signaling. FEMS Microbiol Rev. 2007;31: 425–448.
459 doi:10.1111/j.1574-6976.2007.00072.x
460 3. Glick BR. Modulation of plant ethylene levels by the bacterial enzyme ACC deaminase.
461 FEMS Microbiol Lett. 2005;251: 1–7. doi:10.1016/j.femsle.2005.07.030
462 4. Bangera MG, Thomashow LS. Identification and characterization of a gene cluster for
463 synthesis of the polyketide antibiotic 2,4-diacetylphloroglucinol from *Pseudomonas*
464 *fluorescens* Q2-87. J Bacteriol. 1999;181: 3155–63.
465 5. Pieterse CMJ, de Jonge R, Berendsen RL. The Soil-Borne Supremacy. Trends Plant Sci.
466 2016;21: 171–173. doi:10.1016/j.tplants.2016.01.018
467 6. Haney CH, Samuel BS, Bush J, Ausubel FM. Associations with rhizosphere bacteria can

confer an adaptive advantage to plants. Nat Plants. 2015;1: 15051. doi:10.1038/nplants.2015.51

7. Haney CH, Wiesmann CL, Shapiro LR, Melnyk RA, O'Sullivan LR, Khorasani S, et al. Rhizosphere-associated *Pseudomonas* induce systemic resistance to herbivores at the cost of susceptibility to bacterial pathogens. Mol Ecol. 2017;27: 1833–1847. doi:10.1111/mec.14400

8. Huot B, Yao J, Montgomery BL, He SY. Growth-defense tradeoffs in plants: A balancing act to optimize fitness. Mol Plant. Academic Press, London; 2014;7: 1267–1287. doi:10.1093/mp/ssu049

9. Van Wees SCM, Pieterse CMJ, Trijssenaar A, Van 't Westende YAM, Hartog F, Van Loon LC. Differential Induction of Systemic Resistance in Arabidopsis by Biocontrol Bacteria. Mol Plant-Microbe Interact. The American Phytopathological Society; 1997;10: 716–724. doi:10.1094/MPMI.1997.10.6.716

10. Shah S, Li J, Moffatt BA, Glick BR. Isolation and characterization of ACC deaminase genes from two different plant growth-promoting rhizobacteria. Can J Microbiol. 1998;44: 833–843.

11. Compeau G, Al-Achi BJ, Platsouka E, Levy SB. Survival of rifampin-resistant mutants of *Pseudomonas fluorescens* and *Pseudomonas putida* in soil systems. Appl Environ Microbiol. American Society for Microbiology (ASM); 1988;54: 2432–8.

12. Mohn WW, Wilson AE, Bicho P, Moore ERB. Physiological and Phylogenetic Diversity of Bacteria Growing on Resin Acids. Syst Appl Microbiol. 1999;22: 68–78. doi:10.1016/S0723-2020(99)80029-0

13. Berendsen RL, van Verk MC, Stringlis IA, Zamioudis C, Tommassen J, Pieterse CMJ, et

al. Unearthing the genomes of plant-beneficial *Pseudomonas* model strains WCS358, WCS374 and WCS417. BMC Genomics. BioMed Central; 2015;16: 539. doi:10.1186/s12864-015-1632-z

14. Melnyk RA, Hossain SS, Haney CH. Convergent gain and loss of genomic islands drives lifestyle changes in plant-associated bacteria. bioRxiv. Cold Spring Harbor Laboratory; 2018; 345488. doi:10.1101/345488

15. Hesse C, Schulz F, Bull CT, Shaffer BT, Yan Q, Shapiro N, et al. Genome-based evolutionary history of *Pseudomonas* spp. Environ Microbiol. Wiley/Blackwell (10.1111); 2018;20: 2142–2159. doi:10.1111/1462-2920.14130

16. Lu C-D, Itoh Y, Nakada Y, Jiang Y. Functional analysis and regulation of the divergent spuABCDEFGH-spuI operons for polyamine uptake and utilization in *Pseudomonas aeruginosa* PAO1. J Bacteriol. American Society for Microbiology Journals; 2002;184: 3765–73. doi:10.1128/JB.184.14.3765-3773.2002

17. Imai A, Matsuyama T, Hanzawa Y, Akiyama T, Tamaoki M, Saji H, et al. Spermidine synthase genes are essential for survival of Arabidopsis. Plant Physiol. American Society of Plant Biologists; 2004;135: 1565–73. doi:10.1104/pp.104.041699

18. Lou Y-R, Bor M, Yan J, Preuss AS, Jander G. Arabidopsis NATA1 acetylates putrescine and decreases defense-related hydrogen peroxide accumulation. Plant Physiol. 2016;171: pp.00446.2016. doi:10.1104/pp.16.00446

19. Shah P, Swiatlo E. A multifaceted role for polyamines in bacterial pathogens. Mol Microbiol. 2008;68: 4–16. doi:10.1111/j.1365-2958.2008.06126.x

20. Chen L, Liu Y, Wu G, Zhang N, Shen Q, Zhang R. Beneficial Rhizobacterium *Bacillus amyloliquefaciens* SQR9 Induces Plant Salt Tolerance through Spermidine Production.

514 Mol Plant-Microbe Interact. 2017;30: 423–432. doi:10.1094/MPMI-02-17-0027-R

515 21. Krogh A, Larsson B, von Heijne G, Sonnhammer EL. Predicting transmembrane protein
516 topology with a hidden markov model: application to complete genomes11Edited by F.
517 Cohen. J Mol Biol. 2001;305: 567–580. doi:10.1006/jmbi.2000.4315

518 22. Hanfrey CC, Pearson BM, Hazeldine S, Lee J, Gaskin DJ, Woster PM, et al. Alternative
519 Spermidine Biosynthetic Route Is Critical for Growth of *Campylobacter jejuni* and Is the
520 Dominant Polyamine Pathway in Human Gut Microbiota. J Biol Chem. 2011;286: 43301–
521 43312. doi:10.1074/jbc.M111.307835

522 23. Dieppedale J, Sobral D, Dupuis M, Dubail I, Klimentova J, Stulik J, et al. Identification of
523 a Putative Chaperone Involved in Stress Resistance and Virulence in *Francisella*
524 *tularensis*. Payne SM, editor. Infect Immun. 2011;79: 1428–1439. doi:10.1128/IAI.01012-
525 10

526 24. Tang YP, Dallas MM, Malamy MH. Characterization of the BatI (*Bacteroides*
527 *aerotolerance*) operon in *Bacteroides fragilis*: isolation of a *B. fragilis* mutant with
528 reduced aerotolerance and impaired growth in in vivo model systems. Mol Microbiol.
529 John Wiley & Sons, Ltd (10.1111); 1999;32: 139–149. doi:10.1046/j.1365-
530 2958.1999.01337.x

531 25. Gobert AP, Wilson KT. Polyamine- and NADPH-dependent generation of ROS during
532 *Helicobacter pylori* infection: A blessing in disguise. Free Radic Biol Med. 2017;105: 16–
533 27. doi:10.1016/j.freeradbiomed.2016.09.024

534 26. Marina M, Sirera FV, Rambla JL, Gonzalez ME, Blázquez MA, Carbonell J, et al.
535 Thermospermine catabolism increases *Arabidopsis thaliana* resistance to *Pseudomonas*
536 *viridiflava*. J Exp Bot. 2013;64: 1393–1402. doi:10.1093/jxb/ert012

537 27. Mitsuya Y, Takahashi Y, Berberich T, Miyazaki A, Matsumura H, Takahashi H, et al.
538 Spermine signaling plays a significant role in the defense response of *Arabidopsis*
539 *thaliana* to cucumber mosaic virus. J Plant Physiol. 2009;166: 626–643.
540 doi:10.1016/j.jplph.2008.08.006
541 28. Lou Y-R, Bor M, Yan J, Preuss AS, Jander G. Arabidopsis NATA1 acetylates putrescine
542 and decreases defense-related hydrogen peroxide accumulation. Plant Physiol. 2016;171:
543 pp.00446.2016. doi:10.1104/pp.16.00446
544 29. Liu Z, Beskrovnaya P, Melnyk RA, Hossain SS, Khorasani S, O'Sullivan LR, et al. A
545 Genome-Wide Screen Identifies Genes in Rhizosphere-Associated *Pseudomonas*
546 Required to Evade Plant Defenses. MBio. American Society for Microbiology; 2018;9:
547 e00433-18. doi:10.1128/mBio.00433-18
548 30. Hobley L, Li B, Wood JL, Kim SH, Naidoo J, Ferreira AS, et al. Spermidine promotes
549 *Bacillus subtilis* biofilm formation by activating expression of the matrix regulator *slrR*. J
550 Biol Chem. 2017;292: 12041–12053. doi:10.1074/jbc.M117.789644
551 31. Shelton AN, Seth EC, Mok KC, Han AW, Jackson SN, Haft DR, et al. Uneven
552 distribution of cobamide biosynthesis and dependence in bacteria predicted by
553 comparative genomics. ISME J. Nature Publishing Group; 2018; 1. doi:10.1038/s41396-
554 018-0304-9
555 32. Lamers JG, Schippers B, Geels FP. Soil-borne diseases of wheat in the Netherlands and
556 results of seed bacterization with pseudomonads against *Gaeumannomyces graminis* var.
557 tritici, associated with disease resistance. Cereal Breed Relat to Integr Cereal Prod. 1988;
558 134–139.
559 33. Geels FP, Schippers B. Selection of Antagonistic Fluorescent *Pseudomonas* spp. and their

Root Colonization and Persistence following Treatment of Seed Potatoes. J Phytopathol. Blackwell Publishing Ltd; 1983;108: 193–206. doi:10.1111/j.1439-0434.1983.tb00579.x

34. Howell CR, Stipanovic RD. Control of *Rhizoctonia solani* on Cotton Seedlings with *Pseudomonas fluorescens* and With an Antibiotic Produced by the Bacterium. Phytopathology; 1979;69:480-482.

35. Price MN, Wetmore KM, Waters RJ, Callaghan M, Ray J, Liu H, et al. Mutant phenotypes for thousands of bacterial genes of unknown function. Nature. Nature Publishing Group; 2018;557: 503–509. doi:10.1038/s41586-018-0124-0

36. Rietsch A, Vallet-Gely I, Dove SL, Mekalanos JJ. ExsE, a secreted regulator of type III secretion genes in *Pseudomonas aeruginosa*. Proc Natl Acad Sci. National Academy of Sciences; 2005;102: 8006–8011. doi:10.1073/pnas.0503005102

37. Hanahan D. Studies on transformation of *Escherichia coli* with plasmids. J Mol Biol. Academic Press; 1983;166: 557–580. doi:10.1016/S0022-2836(83)80284-8

Figure 1. Induced Systemic Susceptibility (ISS) is common among closely-related strains of *Pseudomonas* spp. (A) Correlation matrix of new *Pseudomonas* isolates from the Arabidopsis rhizosphere. Isolates were selected based on similarity (>97% identical by partial 16S rRNA) to CH267 (CH235, PB101 and PB103) or distance (<97% identity by partial 16S rRNA) to CH267 (PB120, PB100, PB105). **(B)** Isolates of *Pseudomonas* were tested for their ability to modulate systemic defenses; bars are colored to match the relatedness to CH267 as in (A). Data are the average of 3-5 biological replicates with 2 leaves from each of 6 plants (n=12) per experiment.

582 Letters designate levels of significance ($p<0.05$) by ANOVA and T-test. Isolates from the
583 rhizosphere of Arabidopsis growing in *Massachusetts, USA or #British Columbia, Canada
584
585 **Figure 2. The presence of a genomic island is predictive of the ISS phenotype. (A)** A
586 genomic island identified through comparative genomics is present in the ISS strains CH229,
587 CH235, CH267 and UW4 and absent in Pf0-1 (no effect on systemic defense) and WCS417 (ISR
588 strain). **(B)** Phylogenetic tree based on 122 core *Pseudomonas* genes. Genome sequencing of
589 new strains shows the island is present in strains that enhance susceptibility but not in those that
590 trigger ISR or have no effect. **(C)** Two strains with the island (GW456-L13 and Pf-5) and two
591 without (N1B4 and N2C3) were tested for ISS/ISR. Only those with the island significantly
592 enhanced susceptibility. Data are the average of 3 biological replicates with 2 leaves from each
593 of 6 plants (n=12) per experiment. *$p<0.05$ by ANOVA and T-test. Isolates from the rhizosphere
594 of Arabidopsis growing in *Massachusetts, USA or #British Columbia, Canada
595
596 **Figure 3. Spermidine is necessary and sufficient for ISS. (A-B)** The *speE* gene and the entire
597 gene cluster were deleted from CH267 (A) and UW4 (B). **(C)** Purified spermidine but not
598 spermine applied to the roots of adult Arabidopsis plants is sufficient to trigger ISS. Data are the
599 average of 3 biological replicates with 2 leaves from each of 6 plants (n=12) per experiment.
600 *$p<0.05$ by ANOVA and T-test.
601
602 **Figure 4. *SpeE2* encodes a novel periplasmic spermidine synthase. (A)** The genome of
603 CH267 contains two *speE* homologues. Both contain predicted d-SAM binding domains and a
604 spermidine synthase domain. Only *speE2* contains predicted N-terminal transmembrane

605 domains. **(B)** Protein localization prediction places the polyamine transferase enzyme of *speE2*
606 within the periplasm. **(C)** Spermidine biosynthesis pathways present in *E. coli* and *P.*
607 *aeruginosa*. **(D)** Correlation matrix of spermidine synthase genes in the genomes of 3,886
608 *Pseudomonas* strains. **(E)** The presence of spermidine biosynthesis pathways in *Pseudomonas*
609 genomes.
610
611 **Figure 5. The 11 genes in the ISS locus nearly always co-occur and are present across the**
612 ***Pseudomonas* genus. (A)** Correlation coefficient matrix for the 11 ISS genes across all 3,886
613 *Pseudomonas* genomes in the comparative genomics database. **(B)** Correlation coefficient matrix
614 for the 11 ISS genes across every 50-kb genomic region that contains at least one of the 11
615 genes. **(C)** Distribution of the 11 ISS genes across subclades of the *Pseudomonas* genus. (D)
616 Distribution of the 11 ISS genes within subclades of the *P. fluorescens* group.
617
618 **Figure 6. Conservation of 6 genes from the ISS locus in mammalian pathogens and in**
619 ***Pseudomonas* spp.** Of the 11 genes in the ISS locus, 6 have a paralogous operon that is present
620 in CH267 and most other *Pseudomonas* spp. An operon with a similar configuration is also
621 present in mammalian pathogens and has been implicated in virulence.
622
623 **S1 Table. Unique loci identified in comparative genomics.** The genome content of 4 ISS
624 strains (CH267, CH235, UW4 and CH229) was compared with the closely-related non-ISS strain
625 Pf0-1. 17 predicted protein-coding genes were identified.
626

627 **S1 Figure. Distribution of loci identified by comparative genomics ISS loci across**
628 ***Pseudomonas* strains.** Comparative genomics between ISS strains UW4, CH229, CH235 and
629 CH267 (black arrows) and non-ISS strain Pf0-1 (red arrow) identified 17 predicted protein-
630 coding genes that were absent in Pf0-1 and present in the ISS strains. 11 of these genes were
631 found in a single cluster (box) and were absent in the non-ISS strain WCS365.
632
633 **S2 Figure. The ISS locus is highly variable between closely-related strains**
634 The 11 genes in the ISS locus are present in the ISS strains Pf0-1, CH235, CH267 and CH299
635 but absent in Pf0-1. Genes in the ISS locus are colored as in the key at the bottom of the figure
636 and in Figure 2. Conserved genes not unique to the ISS strains are colored similarly among
637 strains; genes in gray are not conserved between strains at this locus. In CH229, Pf0-1 and
638 CH267 the genes flanking the ISS locus are conserved in the same orientation suggesting a
639 recent insertion or deletion event.
640
641 **S3 Figure. Distribution of *speD/E1* and the *CASDH/C* spermidine biosynthetic pathway**
642 **across *Pseudomonas* species**. While some species contain both pathways (such as *P.*
643 fluorescens) many others (such as *P. putida* or *P. aeruginosa*) contain exclusively the speD/E1 or
644 CASH/C pathway. The number of strains included in each genus is shown in parentheses.
645
646 **S4 Figure. Distribution of *speD/E1* and the *CASDH/C* spermidine biosynthetic pathway**
647 **within subgroups in the *P. fluorescens* clade**. With the exception of Pf-5 which is within *P.*
648 *protegens*, all other ISS strains described fall within *P. madelii*, *P. jessenii* and *P. koreensis*

649 clades as defined by Hesse et al., (2018). The number of strains included in each group is shown

650 in parentheses.

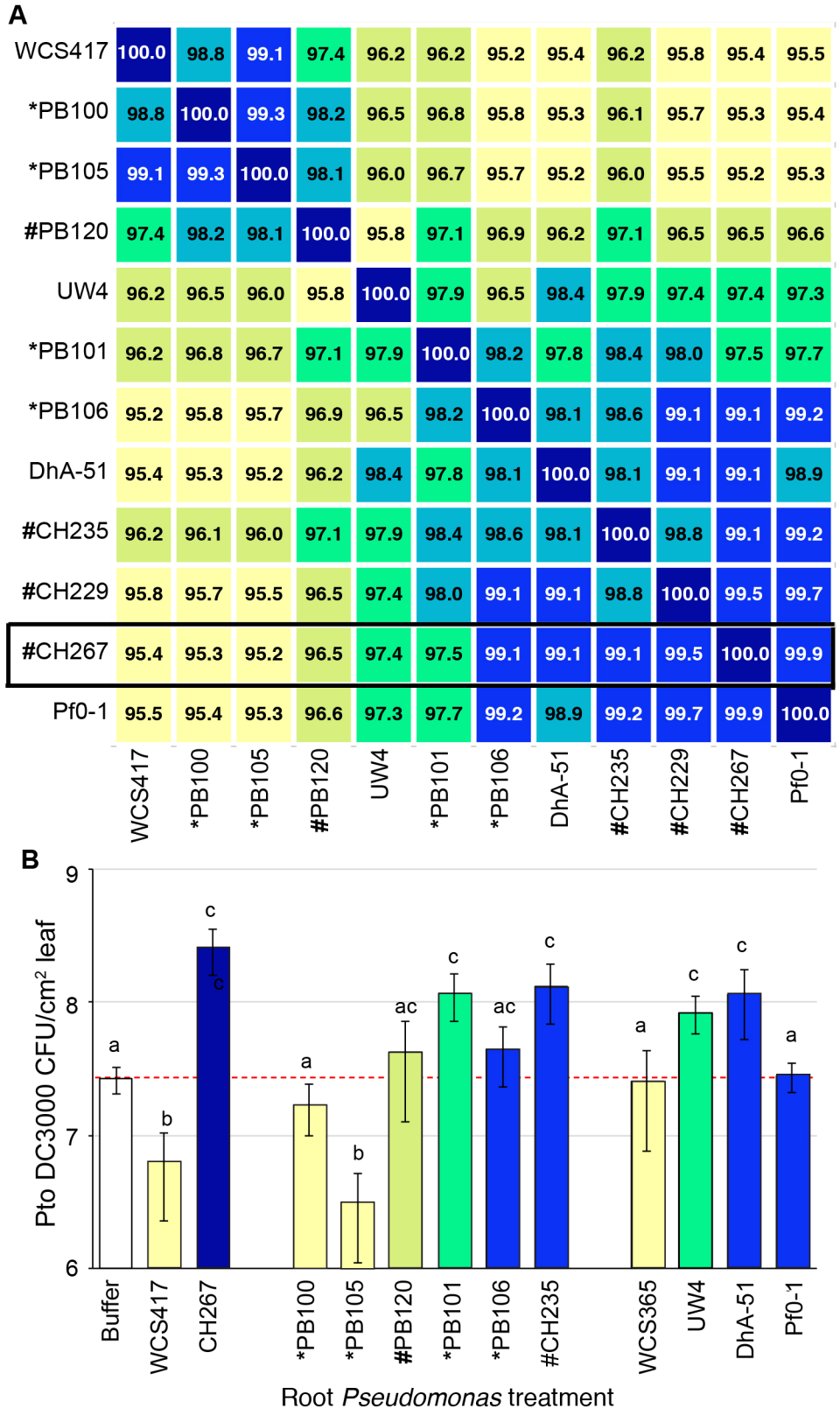
A
WCS417 100.0 98.8 99.1 97.4 96.2 96.2 95.2 95.4 96.2 95.8 95.4 95.5
*PB100 98.8 100.0 99.3 98.2 96.5 96.8 95.8 95.3 96.1 95.7 95.3 95.4
*PB105 99.1 99.3 100.0 98.1 96.0 96.7 95.7 95.2 96.0 95.5 95.2 95.3
#PB120 97.4 98.2 98.1 100.0 95.8 97.1 96.9 96.2 97.1 96.5 96.5 96.6
UW4 96.2 96.5 96.0 95.8 100.0 97.9 96.5 98.4 97.9 97.4 97.4 97.3
*PB101 96.2 96.8 96.7 97.1 97.9 100.0 98.2 97.8 98.4 98.0 97.5 97.7
*PB106 95.2 95.8 95.7 96.9 96.5 98.2 100.0 98.1 98.6 99.1 99.1 99.2
DhA-51 95.4 95.3 95.2 96.2 98.4 97.8 98.1 100.0 98.1 99.1 99.1 98.9
#CH235 96.2 96.1 96.0 97.1 97.9 98.4 98.6 98.1 100.0 98.8 99.1 99.2
#CH229 95.8 95.7 95.5 96.5 97.4 98.0 99.1 99.1 98.8 100.0 99.5 99.7
#CH267 95.4 95.3 95.2 96.5 97.4 97.5 99.1 99.1 99.1 99.5 100.0 99.9
Pf0-1 95.5 95.4 95.3 96.6 97.3 97.7 99.2 98.9 99.2 99.7 99.9 100.0
WCS417
*PB100
*PB105
#PB120
UW4
*PB101
*PB106
DhA-51
#CH235
#CH229
#CH267
Pf0-1
B
Pto DC3000 CFU/cm² leaf
9
8
7
6
a
b
c
c
a
b
ac
c
ac
c
a
c
c
a
Buffer
WCS417
CH267
*PB100
*PB105
#PB120
*PB101
*PB106
#CH235
WCS365
UW4
DhA-51
Pf0-1
Root *Pseudomonas* treatment

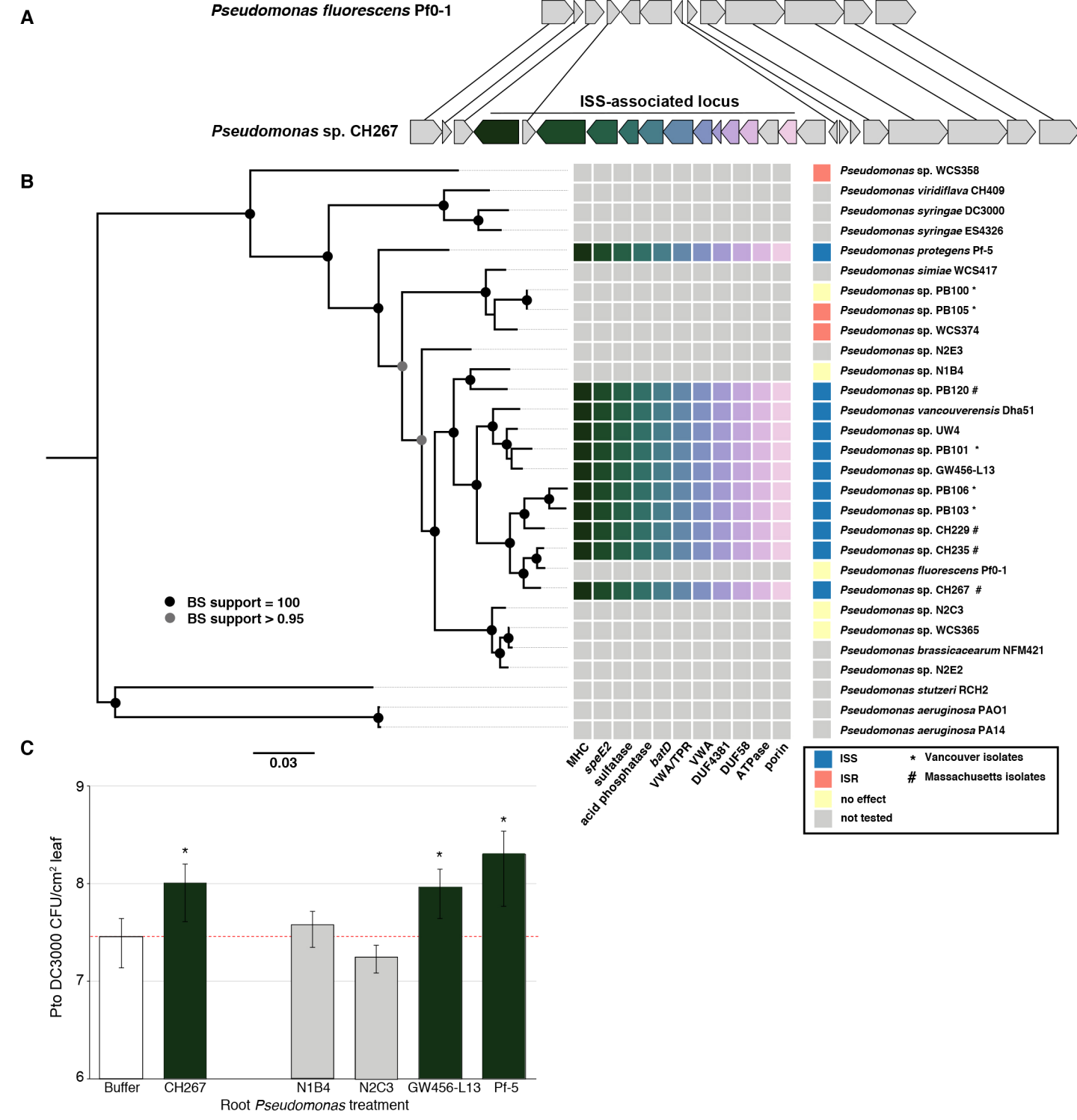
A
Pseudomonas fluorescens Pf0-1
ISS-associated locus
Pseudomonas sp. CH267
B
BS support = 100
BS support > 0.95
0.03
Pseudomonas sp. WCS358
Pseudomonas viridiflava CH409
Pseudomonas syringae DC3000
Pseudomonas syringae ES4326
Pseudomonas protegens Pf-5
Pseudomonas simiae WCS417
Pseudomonas sp. PB100 *
Pseudomonas sp. PB105 *
Pseudomonas sp. WCS374
Pseudomonas sp. N2E3
Pseudomonas sp. N1B4
Pseudomonas sp. PB120 #
Pseudomonas vancouverensis Dha51
Pseudomonas sp. UW4
Pseudomonas sp. PB101 *
Pseudomonas sp. GW456-L13
Pseudomonas sp. PB106 *
Pseudomonas sp. PB103 *
Pseudomonas sp. CH229 #
Pseudomonas sp. CH235 #
Pseudomonas fluorescens Pf0-1
Pseudomonas sp. CH267 #
Pseudomonas sp. N2C3
Pseudomonas sp. WCS365
Pseudomonas brassicacearum NFM421
Pseudomonas sp. N2E2
Pseudomonas stutzeri RCH2
Pseudomonas aeruginosa PAO1
Pseudomonas aeruginosa PA14
MHC
speE2
sulfatase
acid phosphatase
batD
VWA/TPR
VWA
DUF4381
DUF58
ATPase
porin
ISS
ISR
no effect
not tested
* Vancouver isolates
# Massachusetts isolates
C
Pto DC3000 CFU/cm² leaf
9
8
7
6
Buffer
CH267
N1B4
N2C3
GW456-L13
Pf-5
Root Pseudomonas treatment

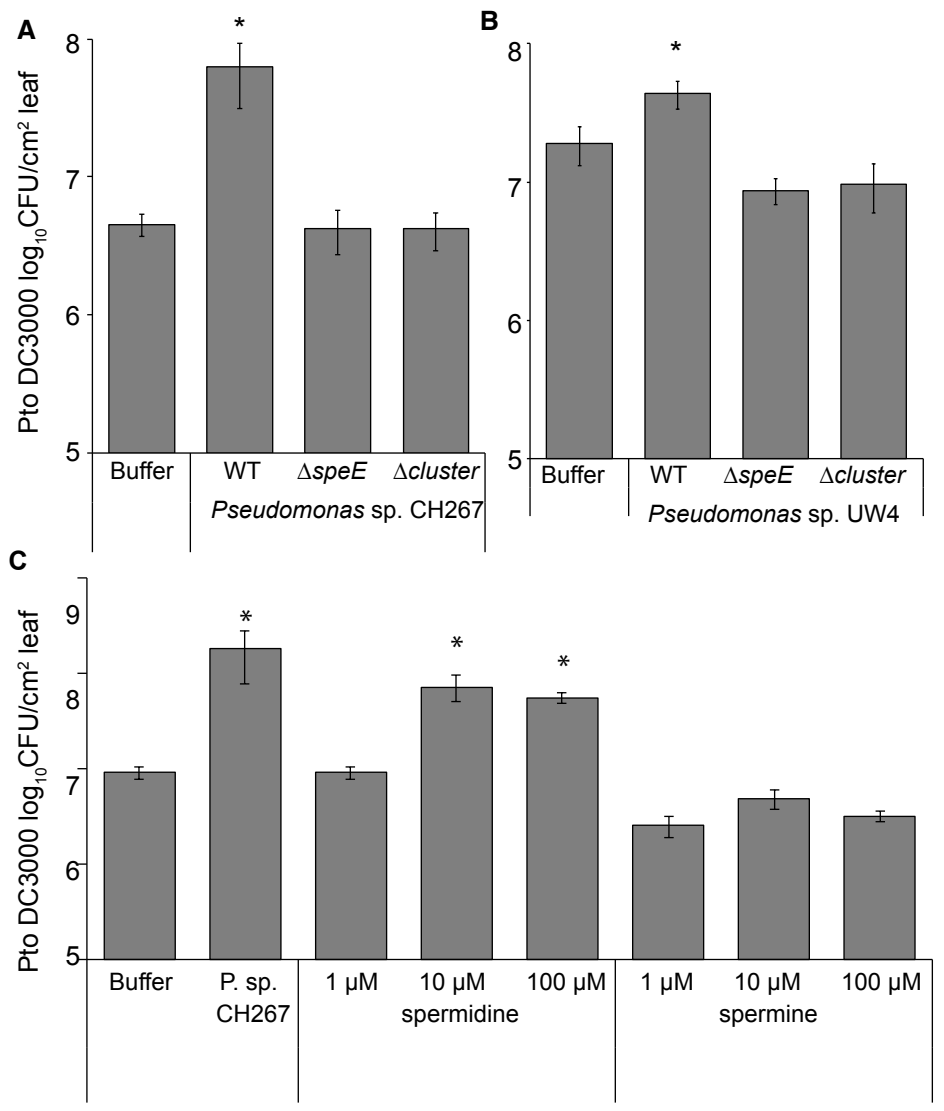
A
B
C
Pto DC3000 log10CFU/cm2 leaf
8
7
6
5
9
*
Buffer
WT
ΔspeE
Δcluster
Pseudomonas sp. CH267
Pseudomonas sp. UW4
P. sp. CH267
1 μM
10 μM
100 μM
spermidine
spermine

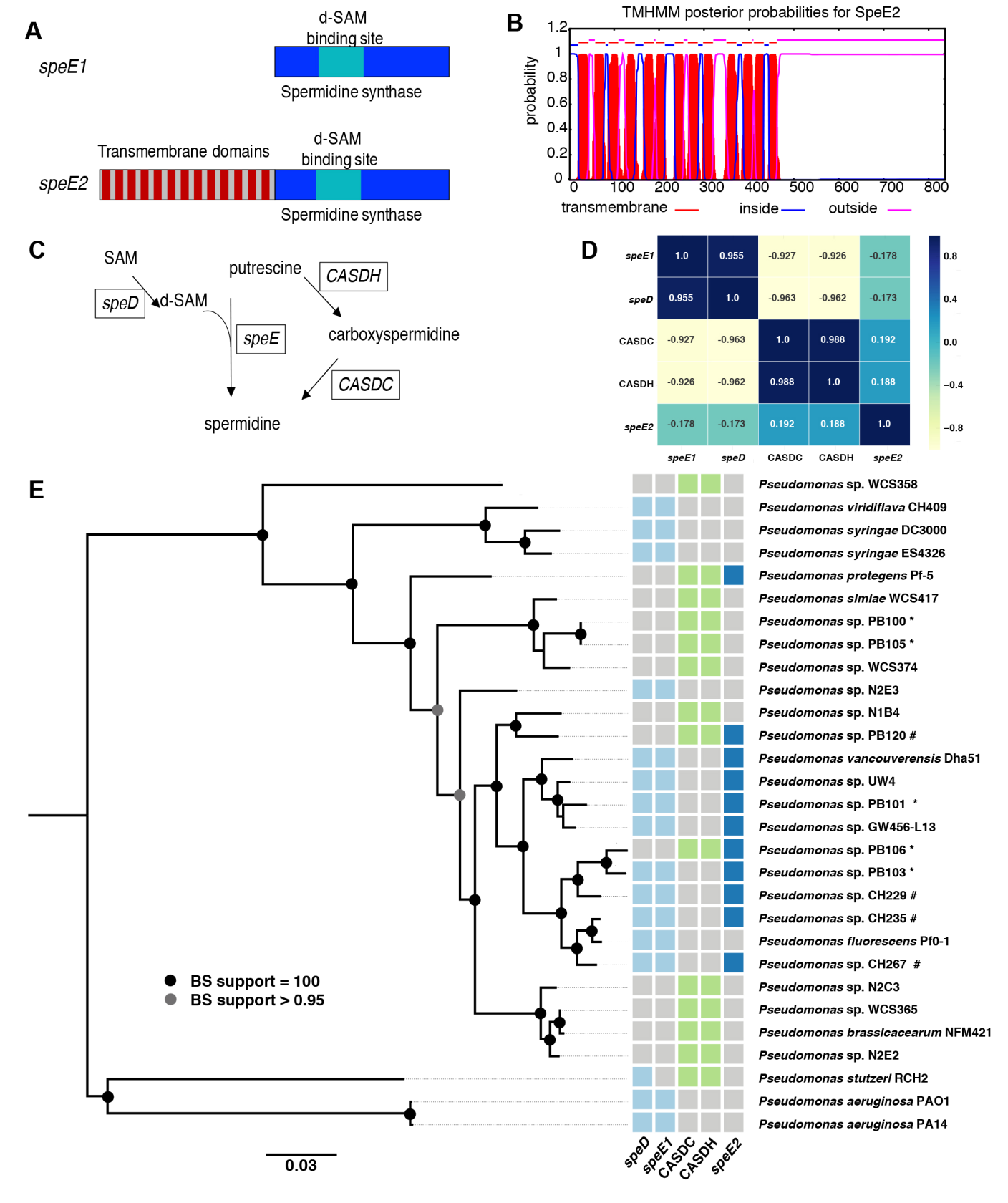
A
speE1
d-SAM binding site
Spermidine synthase
speE2
Transmembrane domains
d-SAM binding site
Spermidine synthase
B
TMHMM posterior probabilities for SpeE2
probability
transmembrane
inside
outside
C
SAM
speD
d-SAM
putrescine
CASDH
speE
carboxyspermidine
CASDC
spermidine
D
speE1
speD
CASDC
CASDH
speE2
E
BS support = 100
BS support > 0.95
0.03
Pseudomonas sp. WCS358
Pseudomonas viridiflava CH409
Pseudomonas syringae DC3000
Pseudomonas syringae ES4326
Pseudomonas protegens Pf-5
Pseudomonas simiae WCS417
Pseudomonas sp. PB100 *
Pseudomonas sp. PB105 *
Pseudomonas sp. WCS374
Pseudomonas sp. N2E3
Pseudomonas sp. N1B4
Pseudomonas sp. PB120 #
Pseudomonas vancouverensis Dha51
Pseudomonas sp. UW4
Pseudomonas sp. PB101 *
Pseudomonas sp. GW456-L13
Pseudomonas sp. PB106 *
Pseudomonas sp. PB103 *
Pseudomonas sp. CH229 #
Pseudomonas sp. CH235 #
Pseudomonas fluorescens Pf0-1
Pseudomonas sp. CH267 #
Pseudomonas sp. N2C3
Pseudomonas sp. WCS365
Pseudomonas brassicacearum NFM421
Pseudomonas sp. N2E2
Pseudomonas stutzeri RCH2
Pseudomonas aeruginosa PAO1
Pseudomonas aeruginosa PA14
speD
speE1
CASDC
CASDH
speE2

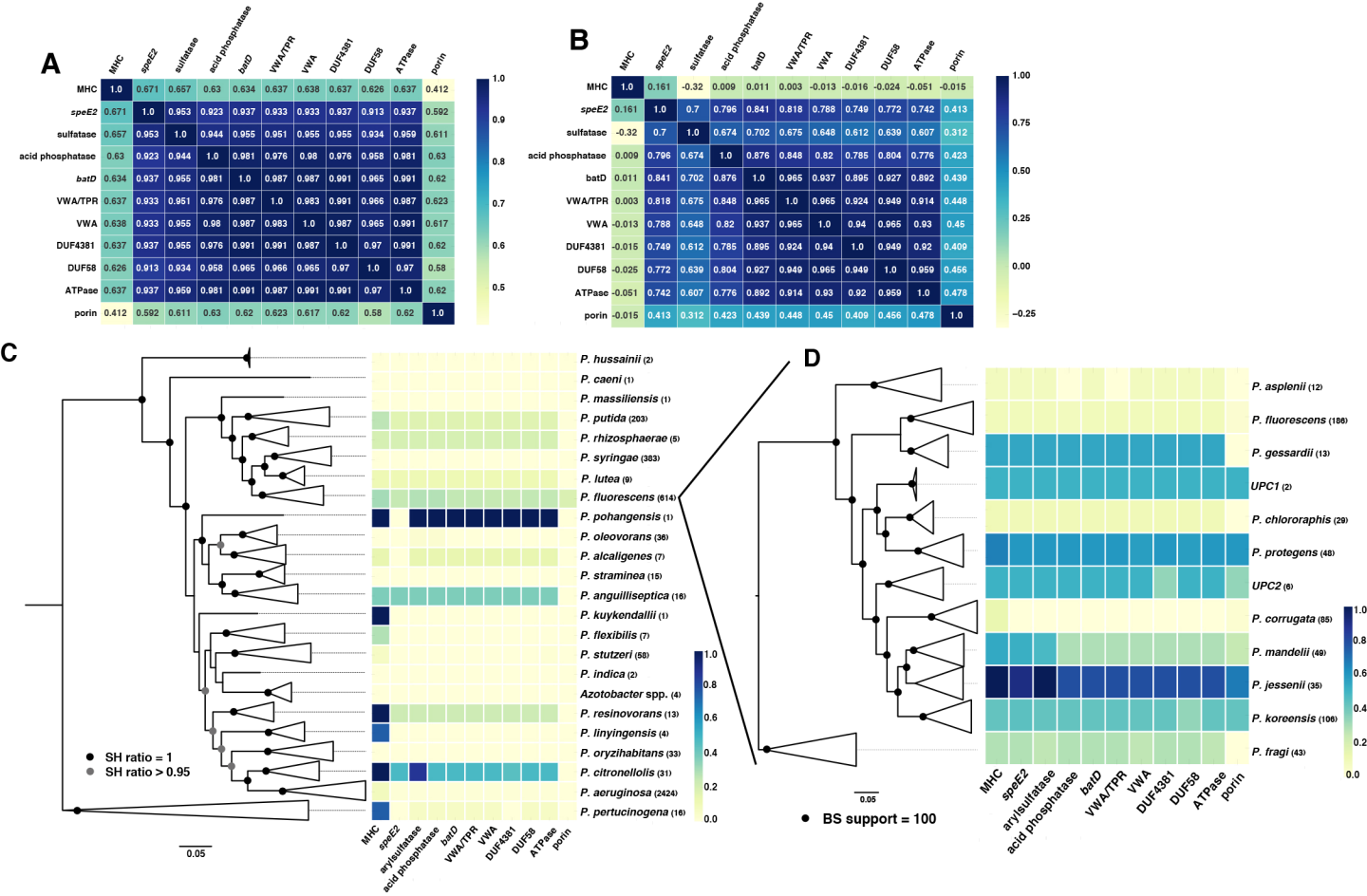
A
MHC speE2 sulfatase acid phosphatase batD VWA/TPR VWA DUF4381 DUF58 ATPase porin
MHC 1.0 0.671 0.657 0.63 0.634 0.637 0.638 0.637 0.626 0.637 0.412
speE2 0.671 1.0 0.953 0.923 0.937 0.933 0.933 0.937 0.913 0.937 0.592
sulfatase 0.657 0.953 1.0 0.944 0.955 0.951 0.955 0.955 0.934 0.959 0.611
acid phosphatase 0.63 0.923 0.944 1.0 0.981 0.976 0.98 0.976 0.958 0.981 0.63
batD 0.634 0.937 0.955 0.981 1.0 0.987 0.987 0.991 0.965 0.991 0.62
VWA/TPR 0.637 0.933 0.951 0.976 0.987 1.0 0.983 0.991 0.966 0.987 0.623
VWA 0.638 0.933 0.955 0.98 0.987 0.983 1.0 0.987 0.965 0.991 0.617
DUF4381 0.637 0.937 0.955 0.976 0.991 0.991 0.987 1.0 0.97 0.991 0.62
DUF58 0.626 0.913 0.934 0.958 0.965 0.966 0.965 0.97 1.0 0.97 0.58
ATPase 0.637 0.937 0.959 0.981 0.991 0.987 0.991 0.991 0.97 1.0 0.62
porin 0.412 0.592 0.611 0.63 0.62 0.623 0.617 0.62 0.58 0.62 1.0
1.0 0.9 0.8 0.7 0.6 0.5
B
MHC speE2 sulfatase acid phosphatase batD VWA/TPR VWA DUF4381 DUF58 ATPase porin
MHC 1.0 0.161 -0.32 0.009 0.011 0.003 -0.013 -0.016 -0.024 -0.051 -0.015
speE2 0.161 1.0 0.7 0.796 0.841 0.818 0.788 0.749 0.772 0.742 0.413
sulfatase -0.32 0.7 1.0 0.674 0.702 0.675 0.648 0.612 0.639 0.607 0.312
acid phosphatase 0.009 0.796 0.674 1.0 0.876 0.848 0.82 0.785 0.804 0.776 0.423
batD 0.011 0.841 0.702 0.876 1.0 0.965 0.937 0.895 0.927 0.892 0.439
VWA/TPR 0.003 0.818 0.675 0.848 0.965 1.0 0.965 0.924 0.949 0.914 0.448
VWA -0.013 0.788 0.648 0.82 0.937 0.965 1.0 0.94 0.965 0.93 0.45
DUF4381 -0.015 0.749 0.612 0.785 0.895 0.924 0.94 1.0 0.949 0.92 0.409
DUF58 -0.025 0.772 0.639 0.804 0.927 0.949 0.965 0.949 1.0 0.959 0.456
ATPase -0.051 0.742 0.607 0.776 0.892 0.914 0.93 0.92 0.959 1.0 0.478
porin -0.015 0.413 0.312 0.423 0.439 0.448 0.45 0.409 0.456 0.478 1.0
1.00 0.75 0.50 0.25 0.00 −0.25
C
P. hussainii (2)
P. caeni (1)
P. massiliensis (1)
P. putida (203)
P. rhizosphaerae (5)
P. syringae (383)
P. lutea (9)
P. fluorescens (614)
P. pohangensis (1)
P. oleovorans (36)
P. alcaligenes (7)
P. straminea (15)
P. anguilliseptica (16)
P. kuykendallii (1)
P. flexibilis (7)
P. stutzeri (58)
P. indica (2)
Azotobacter spp. (4)
P. resinovorans (13)
P. linyingensis (4)
P. oryzihabitans (33)
P. citronellolis (31)
P. aeruginosa (2424)
P. pertucinogena (16)
SH ratio = 1
SH ratio > 0.95
0.05
MHC speE2 arylsulfatase acid phosphatase batD VWA/TPR VWA DUF4381 DUF58 ATPase porin
1.0 0.8 0.6 0.4 0.2 0.0
D
P. asplenii (12)
P. fluorescens (186)
P. gessardii (13)
UPC1 (2)
P. chlororaphis (29)
P. protegens (48)
UPC2 (6)
P. corrugata (85)
P. mandelii (49)
P. jessenii (35)
P. koreensis (106)
P. fragi (43)
0.05
BS support = 100
MHC speE2 arylsulfatase acid phosphatase batD VWA/TPR VWA DUF4381 DUF58 ATPase porin
1.0 0.8 0.6 0.4 0.2 0.0

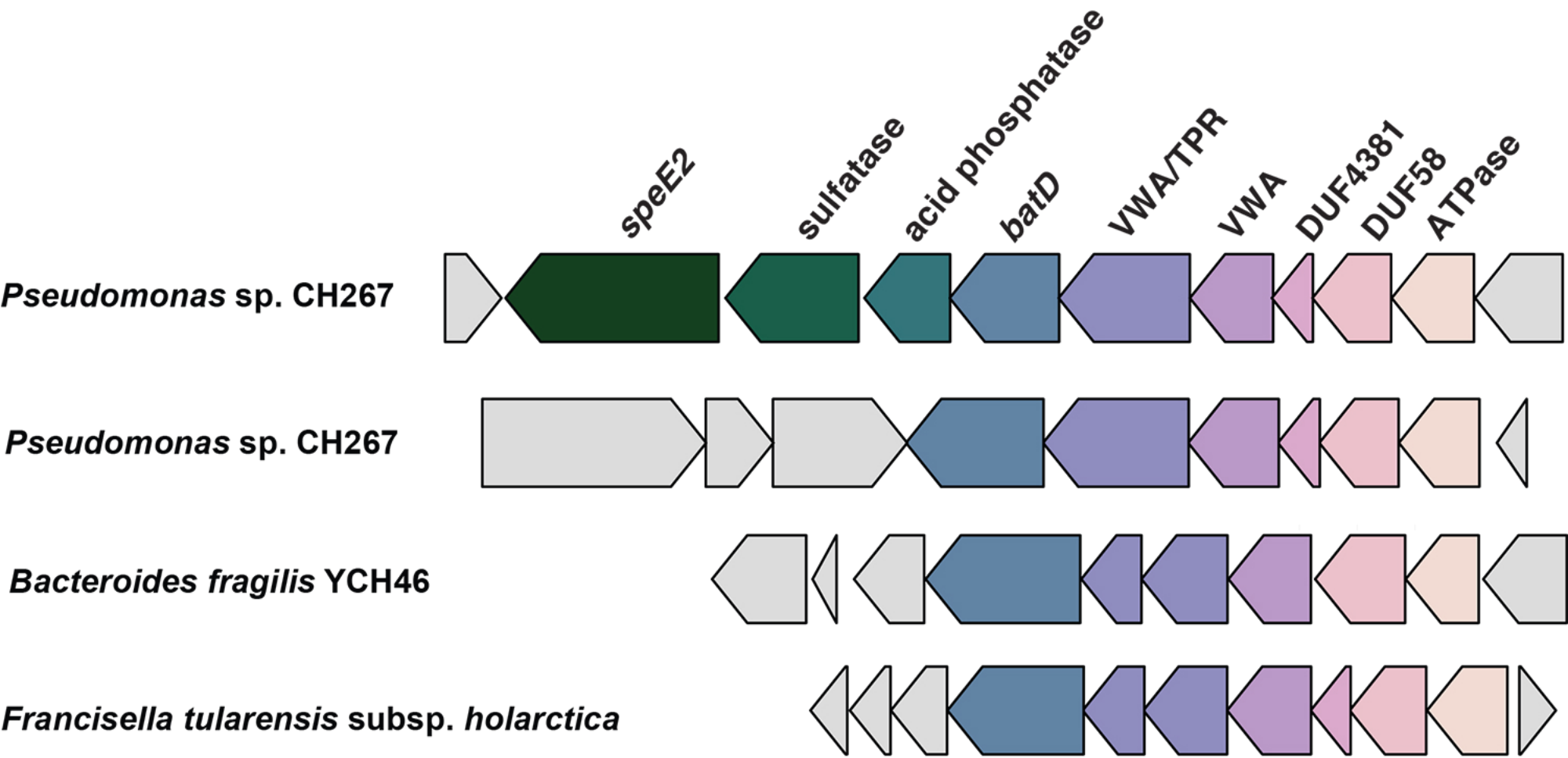
speE2
sulfatase
acid phosphatase
batD
VWA/TPR
VWA
DUF4381
DUF58
ATPase
Pseudomonas sp. CH267
Pseudomonas sp. CH267
Bacteroides fragilis YCH46
Francisella tularensis subsp. holarctica